Kronenberg, Philipp

Working Paper

A high-frequency GDP indicator for Switzerland

KOF Working Papers, No. 518

Provided in Cooperation with:
KOF Swiss Economic Institute, ETH Zurich

Suggested Citation: Kronenberg, Philipp (2024) : A high-frequency GDP indicator for Switzerland, KOF Working Papers, No. 518, ETH Zurich, KOF Swiss Economic Institute, Zurich, https://doi.org/10.3929/ethz-b-000680422

This Version is available at:
https://hdl.handle.net/10419/299396

A High-Frequency GDP Indicator for Switzerland

ETH zürich

KOF

KOF Working Papers

A High-Frequency GDP Indicator for Switzerland

Philipp Kronenberg

No. 518, 06 / 2024

A High-Frequency GDP Indicator for Switzerland*

Philipp Kronenberg¶

KOF Swiss Economic Institute, ETH Zurich

June 25, 2024

Abstract

This paper presents a weekly GDP indicator for Switzerland, which addresses the limitations of existing economic activity indicators using alternative high-frequency data created in the wake of the COVID-19 pandemic. The indicator is obtained from a Bayesian mixed-frequency dynamic factor model that integrates conventional macroeconomic and alternative high-frequency data at weekly, monthly, and quarterly frequencies. By estimating missing observations as latent states through data augmentation, incorporating stochastic volatility in the state equation, and accounting for serial correlation in the measurement errors, the model is able to extract business cycle information from a wide range of data frequencies and capture the large and sudden fluctuations during the COVID-19 pandemic. An empirical application illustrates that the indicator accurately approximates weekly quarter-on-quarter GDP growth for Switzerland and provides valuable information on the trajectory of GDP at high-frequency, especially during crisis periods. Finally, a pseudo-real-time analysis demonstrates credible nowcasts and a fast convergence towards its final version.

JEL Classification: C11, C32, C38, C53, E32, E37
Keywords: Dynamic Factor Model, Business Cycle Index, High-Frequency Data, Economic Activity Indicator, Covid-19

*The author thanks Florian Eckert, Samad Sarferaz, Sylvia Kaufmann, Gabriel Pérez-Quirós, the participants of the Nowcasting Workshop at the Paris School of Economics (2022), the International Symposium of Forecasting (2023), and the Macroeconomic Workshop at the University of Basel (2024) for helpful discussions and comments.

¶Leonhardstrasse 21, 8092 Zurich, kronenberg@kof.ethz.ch.

1 Introduction

During the COVID-19 pandemic, the trajectory of economic activity experienced unprecedented volatility due to the implementation of containment measures, including social distancing, industry shutdowns, and lockdowns. Conventional econometric models failed to accurately capture these sudden and strong movements in economic activity for several reasons. Macroeconomic indicators are typically collected monthly and published with a lag of one month or more. Consequently, they fail to provide timely information on high-frequency economic developments. Additionally, as such large swings have never been recorded in the history of the data, econometric models have not been able to adequately capture these movements, and model estimation has often been heavily biased by these highly influential observations. However, reliable up-to-date assessment of the current economic situation is particularly important for policy making in such situations.

In response to the challenges posed by the COVID-19 pandemic, various methods have been developed to produce accurate forecasts of economic activity under the altered conditions. One approach is to use alternative high-frequency data to approximate economic activity at a higher frequency. Lewis et al. (2020a) and Lewis et al. (2021) introduced the Weekly Economic Indicator (WEI) for the US, which uses the first principal component of a set of high-frequency series to produce a weekly GDP indicator representing the 52-week growth rate of economic activity. This methodology inspired subsequent developments, including the creation of regional economic activity indicators for the US by Baumeister et al. (2024), a weekly GDP indicator for Switzerland by Wegmüller et al. (2023), similar indicators for Austria by Fenz and Stix (2021), and for Italy byDelle Monache et al. (2021). Eraslan and Götz (2021) propose a weekly economic activity indicator for Germany using a mixed-frequency dataset that includes next to weekly high-frequency indicators, industrial production, and GDP. Their approach employs temporal aggregation, as proposed

by Mariano and Murasawa (2003), and an Expectation-Maximization (EM) algorithm to generate a weekly GDP indicator expressed in 13-week growth rates. Adam et al. (2021) followed this approach for the Czech Republic. Alternatively, Woloszko (2020) utilize Google Trends data, while Aprigliano et al. (2023) rely on text-based newspaper data to construct weekly economic activity indicators. The latest contributions address the issue of missing observations in a mixed-frequency set-up. Eckert et al. (2022) propose a mixed-frequency dynamic factor model to produce weekly forecasts of quarter-on-quarter GDP growth rates and employ data augmentation using the precision sampler from Chan and Jeliazkov (2009) and apply temporal aggregation constraints to ensure the summation of weekly GDP growth rates aligning with actual quarterly growth rates. Furthermore, their model also incorporates stochastic volatility in the state equation and serial correlation in the measurement errors, enhancing its flexibility to capture significant economic fluctuations during the COVID-19 pandemic. Eraslan and Reif (2023) apply a similar precision-based sampling approach following Chan et al. (2023).

This paper presents a weekly GDP indicator for Switzerland constructed from a mixed-frequency dynamic factor model that integrates weekly, monthly, and quarterly data from both conventional macroeconomic indicators and alternative high-frequency sources. This model facilitates the near real-time monitoring of GDP by extracting business cycle information from a wide range of data frequencies, thereby enhancing the timeliness and accuracy of economic assessments.

This paper builds on the model proposed by Eckert et al. (2022), a Bayesian mixed-frequency dynamic factor model estimated using three independent state-space blocks. These blocks encompass the estimation of missing observations as latent states through data augmentation, the extraction of dynamic factors, and the estimation of stochastic volatility in the factor state equation. The model estimates the factors conditional on the augmented data, thus enabling the incorporation of alternative high-frequency data de-

spite inherent limitations such as short historical records, high volatility, irregular missing data patterns, publication lags, and varying correlations with actual economic activity. Additionally, the model addresses serial correlation in the measurement errors through quasi-differencing following Chib and Greenberg (1994) to allow the factor to deviate stronger for certain periods.

This paper is the first to apply state-of-the-art methods to deal with missing observations and the extreme observations of the COVID-19 pandemic in a mixed-frequency setup with alternative high-frequency data to produce a weekly GDP indicator. The most comparable contributions are those of Eckert et al. (2022), which focus on nowcasting with multiple factors, and Eraslan and Reif (2023), who also apply a precision sampling approach for the estimation of missing observations in a mixed-frequency dynamic factor model to create a high-frequency GDP indicator, but do not consider any form of stochastic volatility or serial correlation in the errors in order to make the model flexible for accurate estimation during and after the COVID-19 pandemic.

The presented indicator is the first for Switzerland that accurately tracks quarterly GDP growth in high-frequency. In comparison, Wegmüller et al. (2023) develop an indicator reflecting year-on-year GDP growth rates, while the "fever-curve" by Burri and Kaufmann (2020) rather serves as a broad economic sentiment, not directly translatable into GDP growth rates. Other studies that applied alternative high-frequency data for Switzerland include Eckert and Mikosch (2020), who created a mobility tracker that proved effective in indicating sales activity during the COVID-19 pandemic, and Felber and Beyeler (2023), who use transaction payment data for nowcasting GDP with machine learning methods.

In an empirical application, the characteristics of the weekly GDP indicator for Switzerland are presented. An in-sample analysis demonstrates that this indicator accurately captures Swiss GDP dynamics and offers additional insights due to its weekly frequency. An examination of the five most recent economic crises in Switzerland, including the

Great Recession, the European Sovereign Debt Crisis, the Swiss Franc Shock, the German Car Production Shock, and the COVID-19 pandemic, illustrates that the indicator provides valuable information on the trajectory of GDP, especially during periods of abrupt and substantial economic change. It is therefore able to deliver a credible depiction of these crises. A comparison with other high-frequency indicators for Switzerland highlights the distinctive and practical utility of this indicator due to its straightforward interpretability. Additionally, a pseudo-real-time analysis indicates that the indicator generates credible nowcasts from initial estimates and converges towards its final version within a few weeks. Notably, during economic crises, the indicator identifies business cycle turning points relatively early, proving useful for real-time analyses and offering a timely and current overview of the economic situation.

The remainder of this paper is structured as follows. Section 2 presents the model including the three state-space block, the identification of the factor, and the estimation procedure. Section 3 presents an empirical application for Swiss GDP, including a description of the data, the in-sample characteristics of the indicator, a comparison of the indicator with other high-frequency indicators for Switzerland, and a discussion of the real-time properties of the indicator. Finally, Section 4 concludes.

2 Model

This paper adopts the methodology from Eckert et al. (2022) to develop a high-frequency GDP indicator, aiming for optimal in-sample fit and reliable real-time performance. In this paper, the model is constrained to a single factor. This factor is determined by minimizing the error term of the measurement equation for the GDP series, thereby ensuring that the factor closely aligns with the GDP series. As a result, the factor can be interpreted as a high-frequency indicator of GDP. The following chapter presents the

model structure, which is based on the approach of Eckert et al. (2022), but tailored to the use of a single factor and its specific identification.

2.1 Data Augmentation

The model utilizes a collection of n time series with varying frequencies, where t represents the time index of the highest frequency in the dataset. Lower-frequency observations are recorded in the last high-frequency period of the corresponding low-frequency interval, with all other entries set to zero to standardize all time series to the highest frequency. For example, when integrating weekly, monthly, and quarterly data, monthly (quarterly) data are recorded in the last week of each month (quarter) and set to zero elsewhere. If an observation is missing due to publication delays or insufficient historical data, the time series is also assigned a zero value for that period. Consequently, the n-dimensional data vector $\mathbf{y}_t$ generally contains a few actual observations among many zeros. $\mathbf{x}_t$ is an n-dimensional vector that includes real observations and estimated latent observations for variables that are not observed. The relationship between the sparse vector $\mathbf{y}_t$ and the dense vector $\mathbf{x}_t$ is captured by the following identity:

$$\mathbf{y}_t = \mathbf{S}_t \mathbf{x}_t, \tag{1}$$

where $\mathbf{S}_t$ is a diagonal selection matrix of size $n \times n$, with ones on the diagonal where the corresponding value in $\mathbf{y}_t$ is observed, and zeros otherwise. Data augmentation refers to converting the sparse vector $\mathbf{y}_t$ into the dense vector $\mathbf{x}_t$. Thus, Equation (1) is termed the *data augmentation equation*.

2.2 Dynamic Factor

The dynamic factor is defined at a weekly frequency. The *measurement equation for the dynamic factor* f_t is defined as

$$\mathbf{x}_t = \mathbf{L}_0\boldsymbol{\lambda}f_t + \mathbf{L}_1\boldsymbol{\lambda}f_{t-1} + \ldots + \mathbf{L}_s\boldsymbol{\lambda}f_{t-s} + \mathbf{e}_t. \tag{2}$$

s denotes the number of factor lags. The n-dimensional vector $\boldsymbol{\lambda}$ holds the time-invariant factor loadings. The diagonal distributed lag matrices $\mathbf{L}_0, \ldots, \mathbf{L}_s$ contain weights that ensure proper temporal aggregation of the high-frequency factor to the lower-frequency variables in $\mathbf{x}_t$. The model is constrained to a single dynamic factor, which is later identified as the high-frequency growth rate of GDP (see Section 2.5). All time series are stationary and normalized to have a mean of zero and a unit variance. For temporal aggregation of the dynamic factor the geometric mean approximation method initially proposed by Mariano and Murasawa (2003) is applied.[1]

The measurement errors in Equation (2) follow a first-order autoregressive process

$$\mathbf{e}_t = \boldsymbol{\rho}\mathbf{e}_{t-1} + \mathbf{u}_t, \qquad \mathbf{u}_t \sim \mathcal{N}\left(\mathbf{0}, \boldsymbol{\Sigma}\right), \tag{3}$$

where the autoregressive coefficient matrix $\boldsymbol{\rho}$ and the error covariance matrix $\boldsymbol{\Sigma}$ are both assumed to be diagonal and constant over time to maintain a simple model structure.[2]

To estimate the dynamic factor while accounting for serial correlation in the measurement errors, Chib and Greenberg (1994) suggest applying quasi-differencing to the measure-

[1] See for details Appendix B.

[2] Since the dynamic factor model is estimated at weekly frequency, allowing for stochastic volatility in the measurement errors would undermine the model's stability.

ment equation. To do this, the quasi-differenced augmented data vector is defined as

$$\tilde{\mathbf{x}}_t = \mathbf{x}_t - \boldsymbol{\rho}\mathbf{x}_{t-1}. \tag{4}$$

Substituting Equation (2) into Equation (4) results in the *quasi-differenced measurement equation for the dynamic factor*:

$$\tilde{\mathbf{x}}_t = \Big(\mathbf{L}_0\boldsymbol{\lambda}f_t + \ldots + \mathbf{L}_s\boldsymbol{\lambda}f_{t-s}\Big) - \boldsymbol{\rho}\Big(\mathbf{L}_0\boldsymbol{\lambda}f_{t-1} + \ldots + \mathbf{L}_s\boldsymbol{\lambda}f_{t-s-1}\Big) + \mathbf{u}_t, \tag{5}$$

where $\mathbf{u}_t$ is defined in Equation (3) and is serially uncorrelated.[3] The ability to eliminate serially correlated measurement errors through quasi-differencing is feasible because the original measurement equation in Equation (2) uses the augmented dense data vector $\mathbf{x}_t$. This approach allows for managing serial correlation despite the presence of mixed frequencies, missing observations, varying release lags, and differing data histories in the original dataset. By eliminating serial correlation, the common factor can strongly explain the mixed-frequency series during certain periods while being less explanatory during others. This is particularly useful when the data include alternative high-frequency series that fluctuate significantly and are often weakly related to actual economic activity.

The *state equation for the dynamic factor* is given by the autoregressive process

$$f_t = \phi_1 f_{t-1} + \ldots + \phi_p f_{t-p} + e^{h_t}\eta_t, \qquad \eta_t \sim \mathcal{N}(0,1). \tag{6}$$

The autoregressive coefficients are denoted by the scalars $\phi_1, \ldots, \phi_p$, with p indicating the number of lags.[4] The composite error term $e^{h_t}\eta_t$ comprises the time-varying stochastic volatility factor e^{h_t} and the error term η_t following a standard normal distribution.

[3] It is straightforward to rearrange terms in Equation (5) to simplify the estimation of the factor.

[4] To handle unit roots, non-stationary draws of $\phi_1, \ldots, \phi_p$ are excluded, and distant lags of the autoregressive coefficients are shrunk towards zero.

2.3 Stochastic Volatility

The variance of the error term in Equation (6) varies over time to enhance the model's ability to capture periods of heightened volatility, especially during crises. Therefore, the *state equation of the stochastic volatility factor* is represented by the logarithmized stochastic volatility factor which follows a random walk

$$h_t = h_{t-1} + v_t, \qquad v_t \sim \mathcal{N}(0, \omega), \tag{7}$$

Due to the nonlinearities arising from directly solving Equation (6) for h_t, Primiceri (2005) suggest to transform the equation into a linear system through squaring and logarithmic operations. This transformation leads to the subsequent *measurement equation for the stochastic volatility factor*:

$$\log\left((f_t - \phi_1 f_{t-1} - \ldots - \phi_p f_{t-p})^2 + c\right) = 2h_t + \log\left(\eta_t^2\right). \tag{8}$$

An offset constant $c = 0.001$ is introduced to enhance the robustness of the estimation. Since η_t adheres to a standard normal distribution, the error term $\log(\eta_t^2)$ follows a log chi-squared distribution with one degree of freedom, denoted as $\log \chi^2(1)$. To further transform the system into a Gaussian state-space model, the $\chi^2(1)$-distribution is approximated using a mixture of normals, following the methodology outlined in Kim et al. (1998).[5]

[5]See for details Appendix C.8.

2.4 Latent Data

The *measurement equation for the latent dense data vector* $\mathbf{x}_t$ is defined by

$$\mathbf{y}_t = \mathbf{S}_t \mathbf{x}_t + \boldsymbol{\epsilon}_t, \qquad \boldsymbol{\epsilon}_t \sim \mathcal{N}\left(0, \epsilon \mathbf{I}_n\right). \tag{9}$$

The value of ϵ is chosen to be a very small value (10^{-9}), relative to the observed data in $\mathbf{y}_t$, aiming to closely approximate the relationship between observed and augmented data established by Equation (1). As the covariance matrix needs to be invertible in the precision sampling algorithm in the estimation, imposing an exact identity is not feasible. The *state equation for the latent dense data vector* $\mathbf{x}_t$ is obtained by combining Equation (5) and Equation (4) to

$$\mathbf{x}_t = \Big(\mathbf{L}_0 \boldsymbol{\lambda} f_t + \ldots + \mathbf{L}_s \boldsymbol{\lambda} f_{t-s}\Big) - \boldsymbol{\rho}\Big(\mathbf{L}_0 \boldsymbol{\lambda} f_{t-1} + \ldots + \mathbf{L}_s \boldsymbol{\lambda} f_{t-s-1}\Big) + \boldsymbol{\rho} \mathbf{x}_{t-1} + \mathbf{u}_t, \tag{10}$$

with $\mathbf{u}_t \sim \mathcal{N}\left(\mathbf{0}, \boldsymbol{\Sigma}\right)$. The computational complexity stays feasible as the components involving the distributed lag matrices $\mathbf{L}_0, \ldots, \mathbf{L}_s$ can be pre-assigned outside the sampling algorithm.

2.5 Factor Identification and Interpretation

Because the dynamic factor and the factor loadings are unknown, there are infinite ways to interpret the data, a situation known as observational equivalence. To address this issue and identify the factor, certain constraints must be imposed on the parameter space. As outlined by Bai and Wang (2015), the factor loading on GDP, represented as λ_{gdp}, is fixed at unity by using informative priors. This approach resolves the scale and sign indeterminacy typically associated with dynamic factor models. Additionally, rotational

indeterminacy is not an issue in the single factor case. As a result, the dynamic factor is uniquely identified.

One advantage of this methodology is that it provides a clear and intuitive interpretation of the dynamic factor. This is accomplished by applying informative priors to the measurement error for GDP, such that the high-frequency dynamic factor closely approximates the week-on-week growth rate of GDP. Specifically, the autoregressive coefficient ρ_{gdp} are strongly shrunk towards zero and the error term σ_{gdp} on GDP growth is constrained to a small value. This value determines the extent to which the temporally aggregated high-frequency factor can deviate from the observed GDP growth rates.

All other prior distributions are specified uninformative. Nevertheless, stationarity constraints are enforced on the autoregressive coefficients of the dynamic factor. This approach enhances the robustness of convergence during sampling, particularly near turning points.[6]

2.6 Estimation

The estimation process involves estimating the dynamic factor f_t, the stochastic volatility factor h_t, the latent dense data vector $\mathbf{x}_t$, as well as the parameters $\boldsymbol{\lambda}, \phi_1, \ldots, \phi_p$, $\boldsymbol{\rho}$, ω, and $\boldsymbol{\Sigma}$. The joint posterior distribution is simulated using Gibbs sampling. Separate Gibbs sampling blocks are used to estimate f_t, h_t, $\mathbf{x}_t$, and the aforementioned parameters, conditional on the observed data $\mathbf{y}_t$, the selection matrix $\mathbf{S}_t$, and the distributed lag matrices $\mathbf{L}_0, \ldots, \mathbf{L}_s$. To enhance computational efficiency, sparse matrix preallocation and sparse matrix algorithms are employed. Initial values are randomly generated from uniform distributions to ensure robust convergence of the sampler. Convergence of the Gibbs sampling algorithm is evaluated using trace plots and by examining differences in

[6] A detailed explanation of the conditional distributions is provided in Appendix C.

the recursive means of selected parameters. Due to the parsimonious parameterization, a burn-in of 10,000 iterations is sufficient for convergence. Once convergence is achieved, every 5th draw is saved until a sample of 5,000 draws is obtained.

The estimation of f_t, h_t, and $\mathbf{x}_t$ follows the procedure by Chan and Jeliazkov (2009) in the separate Gibbs sampling blocks. The algorithm is extended to handle mixed-frequency data by incorporating the temporal aggregation scheme of Mariano and Murasawa (2003). Appendix C provides the estimation methods for f_t, h_t, $\mathbf{x}_t$ and the remaining parameters $\boldsymbol{\lambda}, \phi_1, \ldots, \phi_p, \omega, \boldsymbol{\rho}$ and $\boldsymbol{\Sigma}$ respectively.

3 Empirical Analysis

3.1 Data

The dataset is compiled to cover a broad range of economic activity in Switzerland. The data covers a period from January 1990 to September 2021. the dataset consists of 53 variables, one sampled quarterly, 26 monthly, one weekly, and 25 daily. Table 1 provides an overview of all the series used in this study, together with meta-information such as frequency, starting date, unit, transformation, and source. The table also categorizes the series into alternative high-frequency data, financial variables, production, labor market variables, retail sales, and business surveys.

The dataset includes 22 daily and one weekly alternative high-frequency series. The aim was to cover a broad range of the economy. Consumer spending is captured by debit and credit card transaction volumes in retail trade, the volume of cash withdrawals at ATMs, passenger frequency in public and private transport, Google mobility data, and Google search hits related to economic conditions and consumer goods purchases. Manufacturing is measured by truck frequency, truck toll from Germany, energy production and con-

sumption volumes, and the frequency of motor vehicles passing through key monitoring stations. Google searches about the perceived labor market situation capture the labor market. The international activity is captured with the number of flight arrivals and departures at the main national airport

In addition to the alternative high-frequency series, the dataset includes three daily and two monthly financial series and 24 monthly macroeconomic series, including business tendency surveys, purchasing manager indices, imports and exports, retail sales, consumer and producer prices, short and long-term interest rates, and stock market indices. These financial and macroeconomic variables are commonly used in the GDP nowcasting literature and cover the most important aspects of the economy. Note that because many of the real indicators in Switzerland, such as industrial production, construction output, or service turnover, are published with a longer delay, survey data is favored in order to obtain better real-time performance of the indicator.

A major challenge for the use of alternative high-frequency data is the limited historical record. However, the model can handle datasets with series starting at different or later dates. This capability results from the treatment of each series as a latent process, regardless of its observation status. Additionally, as alternative high-frequency series may be suspect to structural breaks due to changes in the definition, scope, or coverage of the series, thorough checks have been made.[7] All time series are made stationary and standardized to have a mean of zero and a unit variance.

The daily series in the dataset are aggregated to weekly frequency. This approach simplifies the analysis by avoiding weekly seasonality patterns in the daily series and results in a regular frequency that provides four weekly observations for each of the 12 months, giving a total of 48 weekly observations per year. Temporal aggregation is performed by dividing each month into four approximately equal intervals: days 1 to 7, 8 to 14, 15 to

[7]The notes to Tables 1 indicate which series have been adjusted.

Table 1. Data Overview

Name	Category	Frequency	Release Lag	Start Date	Unit	Transformation	Type	Source
Passenger Car Frequency, Counting Stations on Major Swiss Motorways	Alternative	Daily	1W	2005W2	Actual	Log Difference	Flow	ASTRA
Truck Frequency, Counting Stations on Major Swiss Motorways	Alternative	Daily	1W	2005W2	Actual	Log Difference	Flow	ASTRA
Google Search Index, Perceived Economic Situation	Alternative	Daily	1W	2006W1	Index	None	Stock	trendEcon
Google Search Index, Perceived Labour Market Situation	Alternative	Daily	1W	2006W1	Index	None	Stock	KOF
Truck-Toll Mileage Index, Germany	Alternative	Daily	1W	2008W2	Actual	Log Difference	Flow	Destatis
Energy Consumed by Swiss End Users	Alternative	Daily	1W	2009W2	kWh	Log Difference	Flow	Swissgrid
Energy Production in Switzerland	Alternative	Daily	1W	2009W2	kWh	Log Difference	Flow	Swissgrid
Total Flight Arrivals, Zurich Airport	Alternative	Daily	1W	2011W2	Actual	Log Difference	Flow	Zurich Airport
Total Flight Departures, Zurich Airport	Alternative	Daily	1W	2011W2	Actual	Log Difference	Flow	Zurich Airport
Cash Withdrawals, Swiss-Wide Volume in CHF	Alternative	Daily	1W	2018W2	CHF, in Millions	Log Difference	Flow	SIX Group
Non-Online Retail Sales, Swiss-Wide Volume in CHF	Alternative	Daily	1W	2018W2	CHF, in Millions	Log Difference	Flow	SIX Group
Swiss Debit Card Transactions Abroad, Volume in CHF	Alternative	Daily	1W	2018W2	CHF, in Millions	Log Difference	Flow	SIX Group
Public Transport Passenger Frequency, Zurich Hardbruecke	Alternative	Daily	1W	2019W30	Actual	Log Difference	Flow	SBB
Credit Card Transactions, Swiss-Wide Frequency	Alternative	Weekly	1W	2020W2	Actual, in Thousands	Log Difference	Flow	SPA
Google COVID-19 Community Mobility Reports, Grocery and Pharmacy	Alternative	Daily	1W	2020W2	Percentage	Log Difference	Flow	Google
Google COVID-19 Community Mobility Reports, Parks	Alternative	Daily	1W	2020W2	Percentage	Log Difference	Flow	Google
Google COVID-19 Community Mobility Reports, Residential	Alternative	Daily	1W	2020W2	Percentage	Log Difference	Flow	Google
Google COVID-19 Community Mobility Reports, Retail and Recreation	Alternative	Daily	1W	2020W2	Percentage	Log Difference	Flow	Google
Google COVID-19 Community Mobility Reports, Transit Stations	Alternative	Daily	1W	2020W2	Percentage	Log Difference	Flow	Google
Google COVID-19 Community Mobility Reports, Workplaces	Alternative	Daily	1W	2020W2	Percentage	Log Difference	Flow	Google
Median Day Distance of Representative Swiss Population Sample	Alternative	Daily	1W	2020W2	km	Log Difference	Flow	intervista
Private Transport Frequency, Important Counting Stations, Zurich	Alternative	Daily	1W	2020W2	Actual	Log Difference	Flow	StatistikZH
Public Transport Passenger Frequency, Zurich Main Station	Alternative	Daily	1W	2020W2	Actual	Log Difference	Flow	SBB
10-Year Confederation Bond Yield	Financial	Monthly	5W	1990M1	Percentage	Detrended	Stock	SECO
Swiss Market Index (SMI)	Financial	Daily	1W	1990W1	CHF	Log Difference	Flow	SIX Group
Swiss Stock Market Index, Financials	Financial	Daily	1W	1990W1	CHF	Log Difference	Flow	Datastream
Swiss Stock Market Index, Industrials	Financial	Daily	1W	1990W1	CHF	Log Difference	Flow	Datastream
3-Month CHF LIBOR	Financial	Monthly	5W	1991M12	Percentage	Detrended	Stock	SNB
Consumer Price Index, Total	Prices	Monthly	5W	1990M1	Index, 2015M12=100	Log Difference	Flow	SECO
Producer Prices Index	Prices	Monthly	5W	1990M1	Index, 2015M12=100	Log Difference	Flow	SECO
Consumer Price Index, Excl. Energy, Fresh & Seasonal Products	Prices	Monthly	5W	2000M6	Index, 2015M12=100	Log Difference	Flow	SECO
Gross Domestic Product, Adjusted for International Sport Events	Production	Quarterly	9W	1990Q1	CHF, Real Prices	Log Difference	Flow	SECO
Retail Sales, Culture and Recreation Goods, Constant Prices	Retail	Monthly	9W	2000M2	Index, 2015=100	Log Difference	Flow	SECO
Retail Sales, Food, Beverage and Tobacco	Retail	Monthly	9W	2000M2	Index, 2015=100	Log Difference	Flow	SECO
Retail Sales, Household Equipment	Retail	Monthly	9W	2000M2	Index, 2015=100	Log Difference	Flow	SECO
Retail Sales, Information and Communication Equipment	Retail	Monthly	9W	2000M2	Index, 2015=100	Log Difference	Flow	SECO
Retail Sales, Non-Food	Retail	Monthly	9W	2000M2	Index, 2015=100	Log Difference	Flow	SECO
Retail Sales, Other Goods	Retail	Monthly	9W	2000M2	Index, 2015=100	Log Difference	Flow	SECO
Retail Sales, Total	Retail	Monthly	9W	2000M2	Index, 2015=100	Log Difference	Flow	SECO
Purchasing Managers Index, Manufacturing Sector	Survey	Monthly	5W	1995M1	Index (Diffusion)	None	Stock	Credit Suisse
Purchasing Managers Index, Manufacturing Sector, Backlog of Orders	Survey	Monthly	5W	1995M1	Index (Diffusion)	None	Stock	Credit Suisse
Purchasing Managers Index, Manufacturing Sector, Output	Survey	Monthly	5W	1995M1	Index (Diffusion)	None	Stock	Credit Suisse
Business Situation Assessment, Manufacturing	Survey	Monthly	5W	2004M2	Net Balance	Log Difference	Flow	KOF
Business Situation Assessment, Manufacturing Consumption Goods	Survey	Monthly	5W	2004M2	Net Balance	Log Difference	Flow	KOF
Business Situation Assessment, Manufacturing Durable Goods	Survey	Monthly	5W	2004M2	Net Balance	Log Difference	Flow	KOF
Business Situation Assessment, Manufacturing Intermediate Goods,	Survey	Monthly	5W	2004M2	Net Balance	Log Difference	Flow	KOF
Business Situation Assessment, Manufacturing Investment Goods	Survey	Monthly	5W	2004M2	Net Balance	Log Difference	Flow	KOF
Business Situation Assessment, All Industries	Survey	Monthly	5W	2009M5	Net Balance	Log Difference	Flow	KOF
Business Situation Assessment, Finance & Insurance	Survey	Monthly	5W	2010M8	Net Balance	Log Difference	Flow	KOF
Business Situation Assessment, Construction	Survey	Monthly	5W	2011M5	Net Balance	Log Difference	Flow	KOF
Business Situation Assessment, Project Engineering	Survey	Monthly	5W	2011M5	Net Balance	Log Difference	Flow	KOF
Switzerland, Export: Total, Real, SA, Index (1997=100)	Trade	Monthly	5W	1997M2	Index	Log Difference	Flow	EZV
Switzerland, Import: Total, Real, SA, Index (1997=100)	Trade	Monthly	5W	1997M2	Index	Log Difference	Flow	EZV

***Notes*:** "W" stands for week, "M" for month, and "Q" for quarter. Unless otherwise indicated, all series apply to Switzerland. All monthly series are seasonally adjusted. The release lag for each variable is based on 2020 release schedules. Detrending of a variable is performed by subtracting the rolling in-sample moving average of three times the frequency of the respective variable. During data collection, the following series were adjusted to eliminate structural breaks due to changes in definition, scope, or coverage: Energy Consumed by Swiss End Users, Energy Production in Switzerland, Passenger Car Frequency, and Truck Frequency. Eichenauer et al. (2020) details the methods used for constructing the trendEcon Google search index on perceived economic conditions, which can be found `www.trendecon.org`. The same trendEcon methodology is employed for compiling the Google search index on the perceived labor market situation. *Abbreviations of sources*: ASTRA: Swiss Federal Roads Office, Destatis: German Federal Statistical Office, EZV: Federal Customs Administration, KOF: KOF Swiss Economic Institute, SBB: Swiss federal railways, SECO: Swiss State Secretariat for Economic Affairs, SNB: Swiss National Bank, SPA: Swiss Payment Association, StatistikZH: Statistical Office of the Canton of Zurich.

21, and 22 to the last day. The arithmetic mean of all daily observations within the same interval is then calculated. The same regularisation procedure can be applied to weekly variables in the dataset, as they are linked to specific publication days. This frequency regularisation ensures that the observations are equally spaced and have a consistent frequency.

The release dates of the weekly and monthly series are tracked according to their release schedules in the year 2020. Due to the lack of real-time vintages for the series in the dataset, revisions are not taken into account, making this study a "pseudo" real-time analysis as described by Giannone et al. (2008). Table 1 shows the publication lags for each variable in the dataset. Daily variables are aggregated to weekly frequency. Weekly variables are released the following week. Monthly variables are published in the first week of the following month. And quarterly GDP is published with a nine-week lag.

Figure 1 illustrates the annualized quarter-on-quarter growth rate of Swiss real GDP, adjusted for financial inflows and outflows related to international sporting events, which serves as the target variable.[8]

Since 2005, the Swiss economy has experienced five distinct economic crisis periods or shocks colored in grey: the Great Recession during 2008Q4–2009Q3, the European sovereign debt crisis within 2011Q3–2013Q1, the Swiss franc shock during 2015Q1–2015Q2, the German car production shock during 2018Q3-2018Q4, and the COVID-19 pandemic during 2020Q1–2021Q2. The start and end dates of these crises correspond with periods of quarterly GDP declines or strong recoveries. The crisis periods do not necessarily align with recession periods, which are technically defined as two consecutive quarters of negative GDP growth. During the European sovereign debt crisis, Switzer-

[8]Note that the European Football Association (Uefa) and the International Olympic Committee (IOC) are based in Switzerland. This results in large idiosyncratic movements of GDP. As a result, it is common practice for forecasting to adjust Swiss GDP for financial inflows and outflows related to international sporting events.

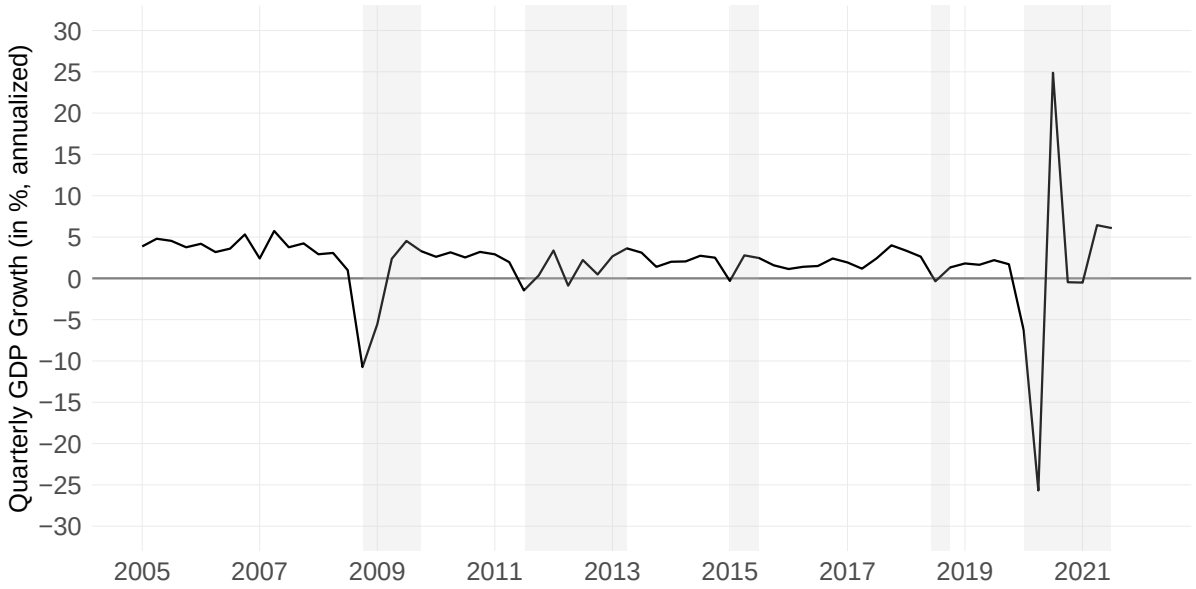

Figure 1: History of Swiss GDP Growth. The figure illustrates the annualized quarter-on-quarter growth rate of Swiss real GDP, adjusted for financial inflows and outflows related to international sporting events, in percent from 2005Q1 to 2021Q3. The crisis periods are indicated by vertical grey bars.

land experienced two non-consecutive quarters of negative growth within a single year. Similarly, during the Swiss franc shock and the German car production shock, Swiss GDP growth turned negative for only one quarter.

3.2 In-sample Characteristics

The weekly indicator resulting from the mixed-frequency dynamic factor model is constructed such that it approximately represents the annualized week-on-week growth rate of GDP (see Section 2). For this reason, the dynamic factor is henceforth referred to as *weekly GDP indicator*. This section studies the in-sample characteristics of the weekly GDP indicator.

The top panel of Figure 2 shows the weekly GDP indicator and its 95%-confidence interval resulting from an ex-post estimation (data available until December 31, 2021). The weekly GDP indicator is shown together with the actual quarter-on-quarter growth rate of GDP, indicated by horizontal red bars.[9] The indicator and the quarter-on-quarter growth rate

[9]The vertical axis of the figure is cropped to allow for an inspection of the fluctuations during normal times. The period of the COVID-19 pandemic will be discussed in greater detail later on.

of GDP match well for the entire history.

The mid panel presents the weekly GDP indicator as an index. Again red bars indicate actual GDP observations. It helps to see how certain periods have permanently weakened the growth path of GDP and helps to put the dimensions of the various crises into perspective. For example, the Great Recession led to a long-term loss of wealth, while the COVID-19 crisis has largely recovered and it has been possible to resume the old growth path.

The lower panel shows the stochastic volatility of the errors in the state equation for the dynamic factor. Time-varying errors allow the factor to account for the higher volatility of economic activity during crisis periods. Indeed, the model uses this flexibility during periods of sudden and strong economic fluctuations, where the volatility of the error term increases.

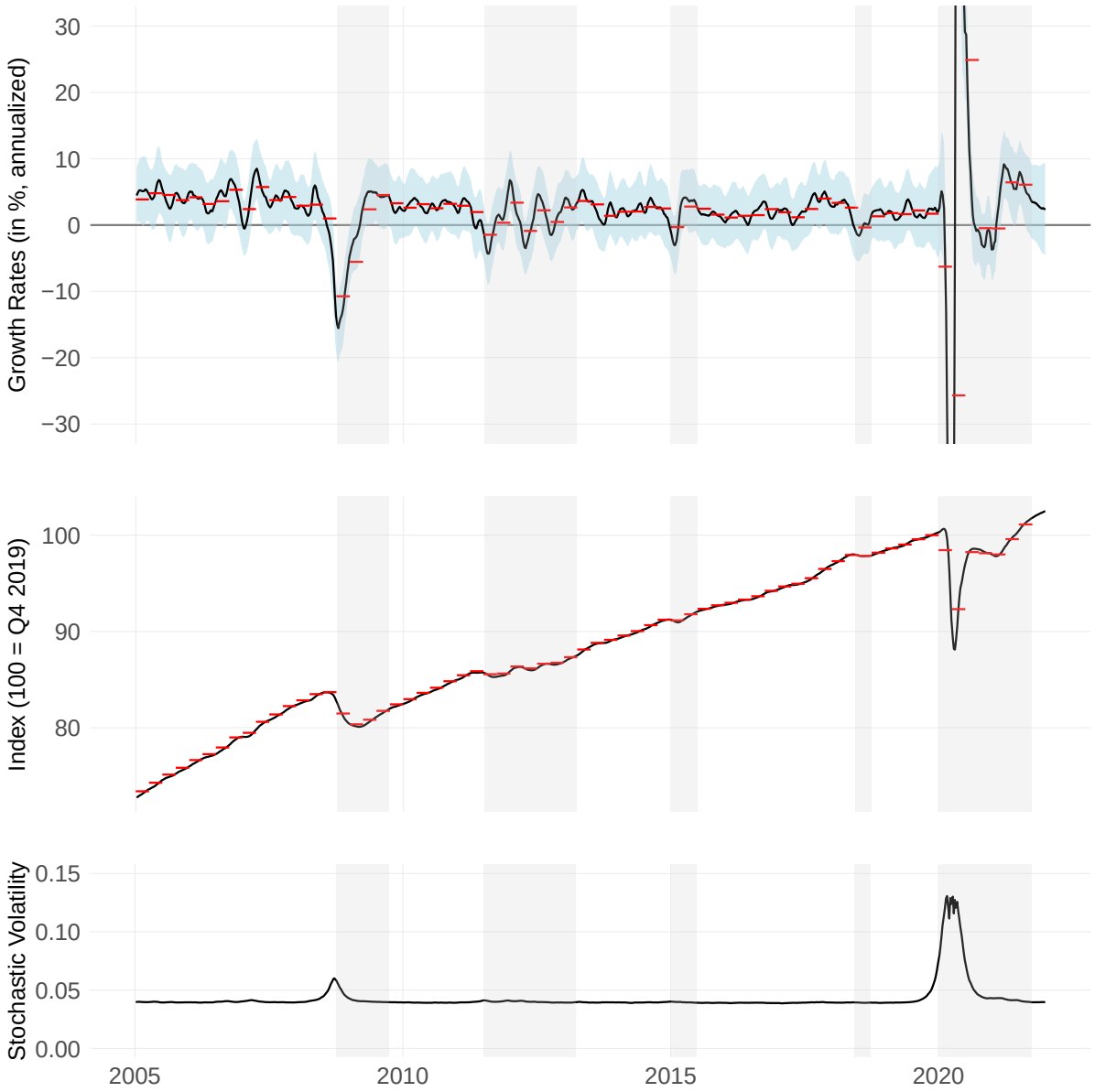

Figure 2: History of Weekly GDP and Stochastic Volatility. The upper panel shows the dynamic factor, representing the annualized week-on-week growth rate of Swiss real GDP, together with a 95%-confidence interval in blue. The estimation is conducted ex post, i.e. based on all data available until December 31, 2021. The red bars indicate the official annualized quarter-on-quarter growth rates of real GDP. The mid panel shows the weekly GDP indicator as an index, normalized by its value in Q4 2019. The red bars indicate the official real GDP observations. The lower panel shows the estimated stochastic volatility. Periods classified as economic crisis are indicated by vertical grey bars. The vertical axis of the upper panel is truncated to allow for an appropriate assessment of the entire history.

The previously presented alternative high-frequency data are especially useful in times of sharp and strong downturns and rebounds, as they should capture the increased volatility faster and to a greater extent than conventional macroeconomic data. To study this, a special emphasis is put on the five economic crises in Switzerland since the year 2005.

Figure 3 presents a more detailed view of the weekly GDP indicator during the before-

mentioned crisis periods. Again the annualized weekly growth rates with 95%-confidence intervals in blue are illustrated together with the realized annualized quarter-on-quarter growth rate of GDP in red. The crisis quarters are indicated with vertical grey bars.

During the Great Recession, the indicator showed negative growth rates from the last week of July 2008, reaching a low in mid-October of about -15%. From March 2009, weekly growth rates returned to positive territory. Overall, GDP experienced 30 consecutive weeks of negative growth. The evolution of these weekly growth rates shows that both the downturn and the subsequent recovery were stronger than the quarterly GDP observations would suggest.

During the European sovereign debt crisis, Switzerland experienced a significant degree of economic volatility over several quarters including several negative or almost stagnating quarterly GDP growth rates. This was driven by several factors, including the appreciation of the Swiss franc, heightened uncertainty, and highly volatile transit trade. The weekly GDP indicator indicates that weekly GDP experienced negative growth in the third quarter of 2012, which would have been missed by quarterly observations.

On 15 January 2015, the Swiss National Bank (SNB) unexpectedly abandoned the minimum exchange rate of 1.20 Swiss francs per euro. This resulted in a swift appreciation of the Swiss franc, which has been referred to as the "Swiss franc shock". This event led to a 0.7% decline in GDP during the first quarter of 2015, followed by a robust growth of 2.7% in the subsequent quarter. The weekly GDP indicator indicates that the economic downturn following the shock was pronounced reaching -3%, but a sharp recovery commenced by the end of February, mitigating a more severe contraction for the first quarter of 2015 in quarterly numbers.

In the third quarter of 2018, Switzerland experienced a decline in GDP growth, followed by a period of relatively weak GDP growth. This was in part due to the introduction of

the new emission testing standard WLTP ("Worldwide Harmonized Light Vehicles Test Procedure") in the EU in September 2018. As a consequence of the fact that a significant number of vehicle types had not yet been certified by the deadline, inventories were increased to a considerable extent, and production was temporarily halted. Consequently, German GDP declined by 0.8%. The postponement of the approval of new German automobile models had an impact on Swiss suppliers of vehicle parts and metals, as well as on the sale of new vehicles. The new standard in the automotive industry had long-term effects on the entire sector, resulting in rather weak growth in the forthcoming quarters. Furthermore, exports of chemicals and pharmaceuticals experienced a pronounced decline in the third quarter, which was offset in the first month of the fourth quarter. This suggests a temporal shift in foreign deliveries.

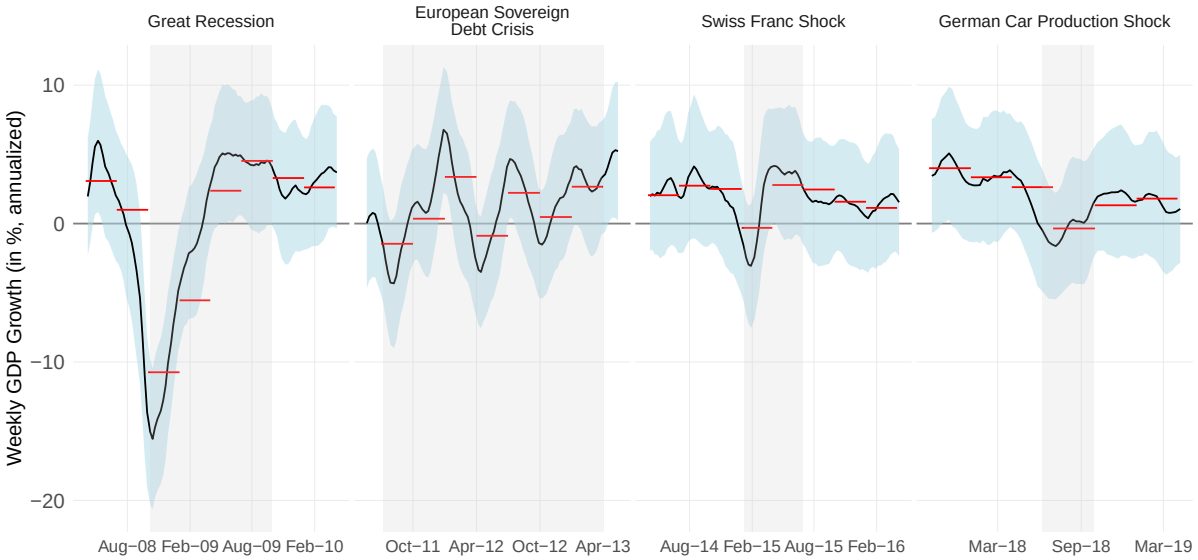

Figure 3: Weekly GDP Growth During Crisis Periods. Notes: See Figure 2.

Figure 4 focuses on the period of the COVID-19 pandemic, which represented a profound and abrupt shock to the Swiss economy. The figure illustrates the weekly GDP indicator along with a 95% confidence interval and the actual quarter-on-quarter GDP growth rate. Important policy decisions during the pandemic are marked by vertical dotted lines. Appendix A details the timing and presents a list of measures implemented by the Swiss federal government. The first COVID-19 infection in Switzerland was reported on

February 25, 2020. Restrictions on events and gatherings were gradually intensified from late February through early March. On March 16, the government imposed a nationwide lockdown in response to the widespread transmission of the virus. The weekly GDP indicator shows a significant decline in economic activity even before the lockdown, which can be attributed to a reduction in mobility and consumption by the population from late February onwards in reaction to the pandemic's spread (e.g., Eckert and Mikosch, 2020).

Companies cut back on production, as evidenced by a marked increase in claims for short-term work. The lockdown intensified the economic downturn, which reached its low point at the end of March. As infection rates fell rapidly in April, public life resumed and businesses and schools reopened on 29 April, leading to a rapid economic recovery. From May, weekly GDP growth declined again and briefly turned negative in early October due to a resurgence of COVID-19 cases. On 19 October, the government reintroduced stricter social distancing measures. In December and January, partial closures were reimposed. However, the economic impact of these measures was minimal compared to the lockdown in spring 2020. With the acceleration of the vaccination campaign and the free availability of COVID-19 tests, economic activity returned to positive growth rates in early 2021. Despite a resurgence of COVID-19 infections in the winter of 2021, driven by the rapid spread of the Omicron variant, economic activity remained largely unaffected and continued to normalize throughout the rest of 2021.

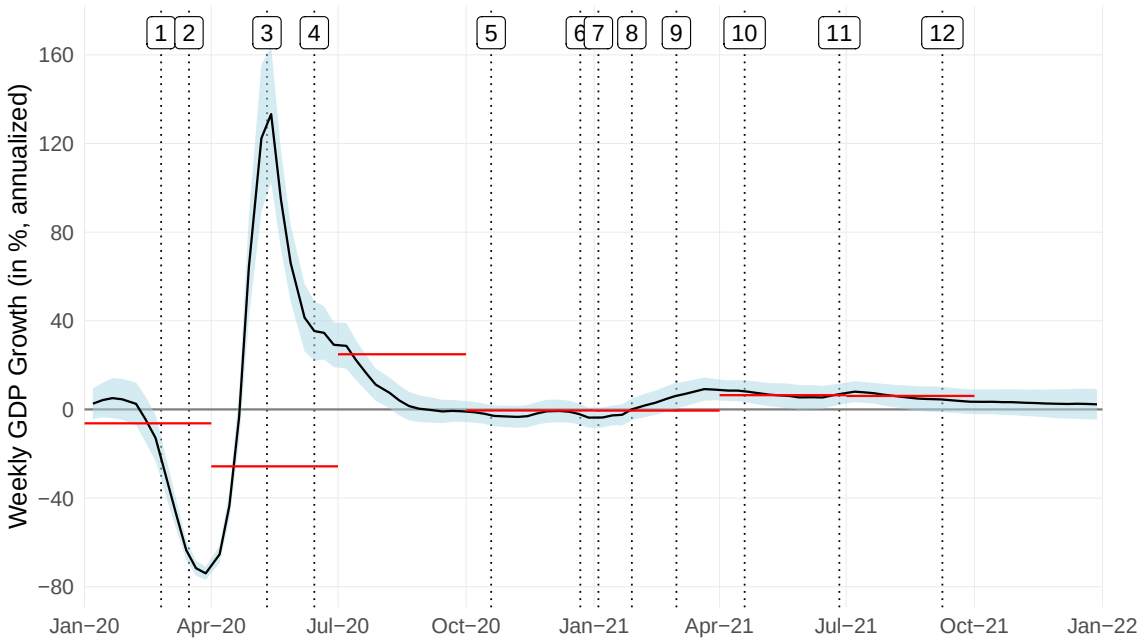

1: First Confirmed Corona Case
2: First Nationwide Lockdown
3: Reopening of Stores & Schools
4: Reopening of Borders
5: Retightening of Social Distancing Rules
6: Second Nationwide Lockdown
7: Begin Vaccination Campaign
8: Free COVID−19 Tests Available
9: Reopening of Stores & Public Facilities
10: Reopening of Outdoor Restaurants
11: Easing of Social Distancing Measures
12: COVID−19 Certificate Obligation

Figure 4: Weekly GDP Growth During the COVID-19 Pandemic. Notes: See Figure 2.

3.3 Comparison to other High-frequency Indicators

During the COVID-19 pandemic, there was a high demand for high-frequency information on the current state of the Swiss economy. Accordingly, there have been several attempts to produce a high-frequency indicator of Swiss economic activity. The following section compares the existing high-frequency indicators for Switzerland.

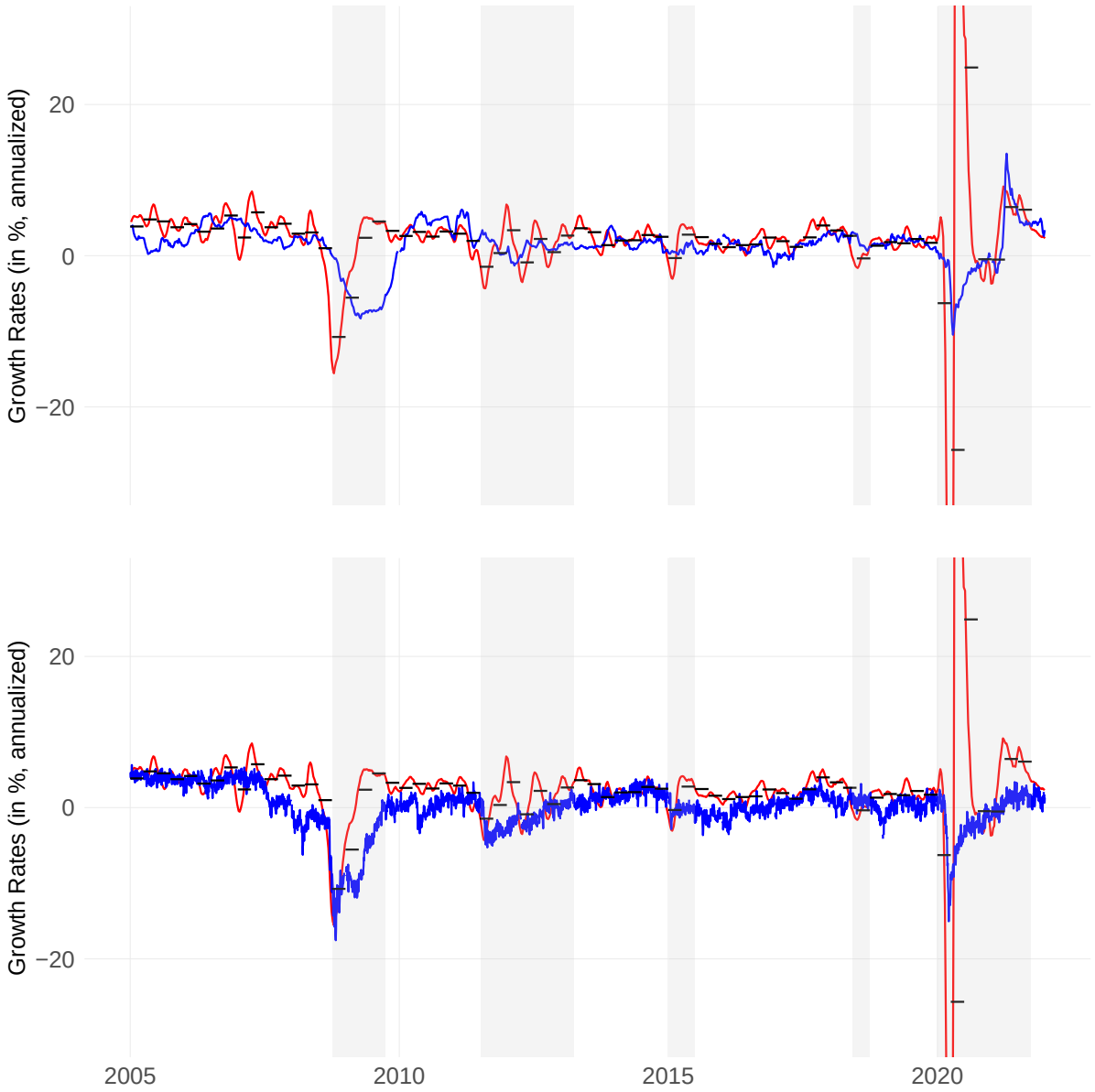

Figure 5: History of other Weekly GDP Indicators. The upper panel shows the weekly GDP indicator, representing the annualized week-on-week growth rate of Swiss real GDP, in red and the weekly activity indicator from SECO by Guggia et al. (2020) in year-on-year growth rates in blue. The black bars indicate the official annualized quarter-on-quarter growth rates of real GDP. The lower panel shows the standardize and inverted fever curve from Burri and Kaufmann (2020). Periods classified as economic crisis are indicated by vertical grey bars. The vertical axis is truncated to allow for an appropriate assessment of the entire history.

The upper panel of Figure 5 shows the weekly GDP indicator, representing the annualized week-on-week growth rate of Swiss real GDP, in red and the weekly activity indicator (WWA) from SECO by Guggia et al. (2020) in year-on-year growth rates in blue. The black bars indicate the official annualized quarter-on-quarter growth rates of real GDP. SECO's Weekly Activity Index was created during the COVID-19 pandemic to provide faster information on the current economic situation in Switzerland. It follows the exam-

ple of Lewis et al. (2020b) and uses only alternative high-frequency data, as conventional economic indicators were not suitable for capturing events timely. The weekly activity indicator uses similar high-frequency data as the weekly GDP indicator described in this paper, including cash withdrawals, card transactions, electricity consumption, air pollution, net tonne-kilometers by rail, registered unemployment, sight deposits at the Swiss National Bank and exports and imports of goods. All series are aggregated to a weekly frequency and adjusted for seasonality and outliers. Finally, a factor is constructed from the growth rates of the data using principal components. The indicator is scaled to show the growth rate compared to the same quarter of the previous year.

The figure shows that the weekly activity indicator from SECO measures something different from the weekly GDP indicator presented in this paper, as the weekly activity indicator from SECO shows the year-on-year growth rate and not the quarter-on-quarter growth rate of GDP. This can also be seen when comparing the development of the indicator with the quarter-on-quarter GDP growth rates. This is particularly evident in times of crisis, such as the Great Recession or the COVID-19 pandemic, when the two measures diverge significantly.

The lower panel of Figure 5 shows again the weekly GDP indicator, representing the annualized week-on-week growth rate of Swiss real GDP, in red and the standardized inverted "fever curve" by Burri and Kaufmann (2020) in week-on-week growth rate in blue. The fever curve is described as an indicator that provides a timely assessment of the economic health of the Swiss economy. It provides a high-frequency sentiment indicator, as it is constructed from daily financial and news data, and therefore provides an early warning signal, especially during crisis periods. The indicator uses data such as bond yields, term spreads, interest rate differentials, corporate risk premia, stock market volatility, and news sentiment. News sentiment was extracted from the headlines and lead texts of the largest Swiss newspapers. A factor was then extracted from the data

using principal components.

The graph shows that the fever curve in general follows the quarterly GDP growth rates. However, there are significant deviations in different periods. Moreover, the indicator does not reflect the quarterly growth rates of GDP but rather provides a sentiment. In this way, it can provide an early signal for crisis periods but does not necessarily move in the same scale as GDP does. This is particularly evident during the COVID-19 pandemic when the indicator does not adequately reflect the extent of the downturn and does not capture the subsequent recovery at all. Similarly, during the Great Recession, the European sovereign debt crisis, or the Swiss franc shock, the indicator cannot exactly reproduce the expected evolution of quarterly GDP growth.

A comparison with existing high-frequency indicators shows that neither provides an accurate picture of the quarter-on-quarter growth rate of Swiss GDP. While both indicators are measured on a different scale, they also have technical limitations. Both indicators use only alternative high-frequency data without incorporating information from conventional economic indicators relevant for GDP estimation. The weekly GDP indicator described in this paper uses alternative high-frequency data as well as conventional economic data. Its methodological construction ensures that it accurately represents the quarter-on-quarter GDP growth rate. This has several advantages for policy decisions, as the quarter-on-quarter GDP growth rate is an important measure of a country's economic development.

3.4 Real-time Properties

The previous analysis showed that the weekly GDP indicator is able to capture ex-post fluctuations in economic activity well. However, the real-time performance of the indicator may be different, as it is subject to revisions caused by new information from

subsequent data releases. To this end, the real-time properties of the indicator are assessed in a pseudo-real-time exercise by estimating the model recursively from January 2005 to December 2021 at a weekly frequency. Data availability is reconstructed to historical vintages according to the publication dates described in Table 1, while potential data revisions are not taken into account.

Figure 6 illustrates the weekly GDP indicator from its initial release to its 30th version, spanning the period from 2005 to 2021. The initial release for any given week t serves as the real-time estimate for that week, incorporating only the data available up to week t. For example, the real-time estimate for the first week of 2020 comprises solely data that had been published up to the end of that week. Conversely, the 30th release version for any week t incorporates data published up to the 29th week following week t.

As illustrated in the figure, earlier releases indicated in yellow exhibit more pronounced fluctuations compared to later releases shown in red and blue, particularly during periods of crisis. Additionally, the yellow lines frequently lag behind the red and blue lines. This suggests that earlier releases tend to respond more slowly to macroeconomic fluctuations than later releases. The initial estimates are primarily based on alternative and financial high-frequency series, which are the most immediately available data in the dataset. In contrast, later releases incorporate monthly series and actual quarterly GDP figures.[10] The later published macroeconomic variables help to correct any potentially misleading or overstated signals from the high-frequency alternative and financial data. In general, only a few revisions are necessary for the indicator to align closely with the stable state depicted in the subsequent releases.

A more detailed examination of the Great Recession reveals that the model required a relatively lengthy period of adjustment. One possible explanation for this is that it was the first significant economic crisis in the sample period, and the model lacked

[10]See Table 1 for the release lag of each variable.

comparable data at the time. Secondly, at the time, only a limited number of high-frequency indicators were available for use in the model, the majority of which were financial variables. Consequently, the model was only able to utilize these in its early vintages. Subsequently, during the COVID-19 pandemic, the model demonstrated a markedly accelerated adjustment, as it had already acquired the capacity to learn from past crisis periods and as the dataset encompassed a substantial number of high-frequency indicators that captured the fluctuations during this period.

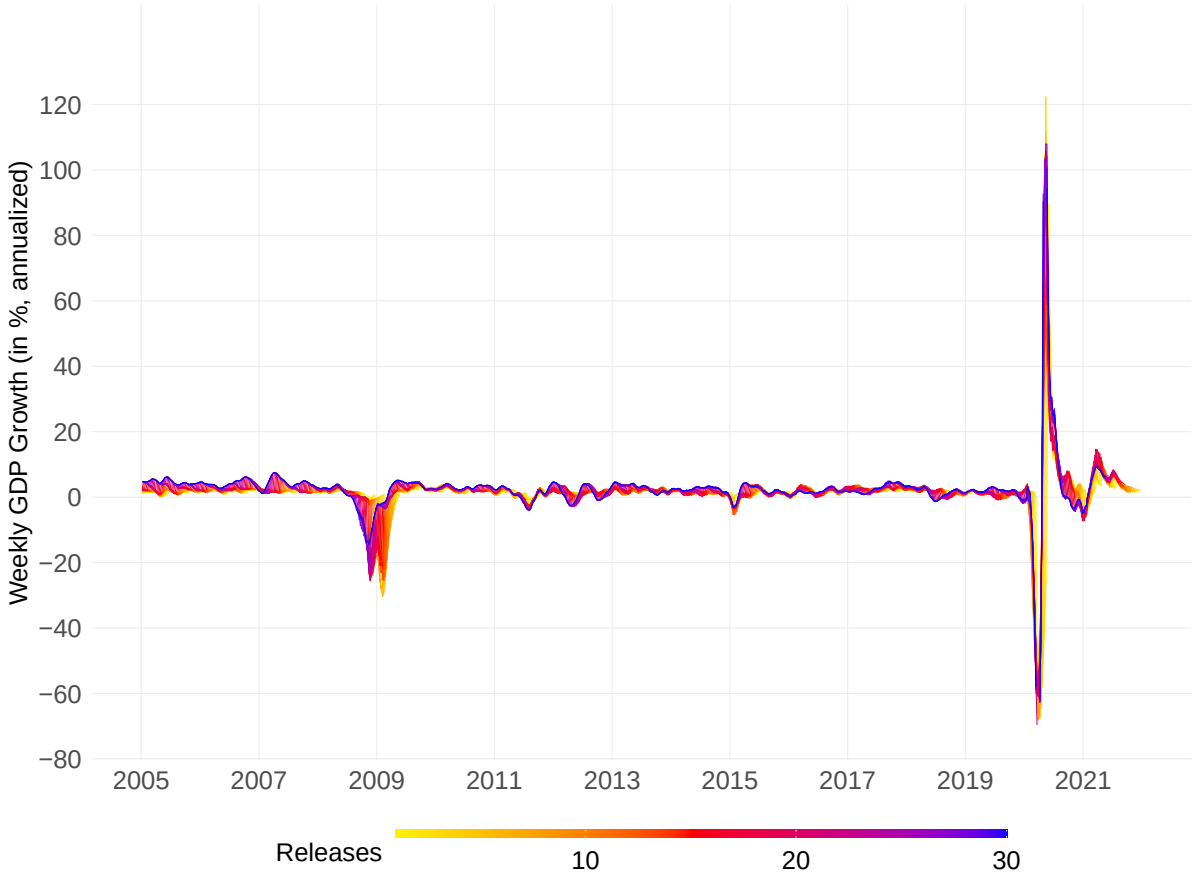

Figure 6: Revisions of the Weekly GDP Indicator. The figure compares the weekly GDP indicator for different releases. The color bar goes from the first release in yellow over the 15th release in red to the 30th release in blue. The sample ranges from 2005 to 2021.

To assess the real-time performance of the weekly GDP indicator, the indicator using different information sets are compared. Figure 7 compares the indicator based on the most recent data vintage (including all data released up to 31 December 2021) with its first release version (the "real-time indicator") and the version using data available

approximately one month after the reference period (i.e. for each week t, the indicator as published in week $t + 4$, including all data available up to week $t + 4$). The real-time version of the indicator relies exclusively on alternative and financial high-frequency data for its weekly estimates of GDP growth, as other variables are published with a time lag.

The figure shows that while the real-time indicator generally reflected the crisis effectively, it lagged behind the most recent indicator release in capturing the fluctuations in 2020 and 2021. In particular, it detected the onset of the severe downturn in early 2020 in mid-March rather than in late February. In addition, the real-time indicator detected the recovery in April and May later than the latest release, initially underestimating both the depth of the trough in March and the magnitude of the rebound in May. However, the annualization of the weekly GDP growth rates visually exaggerates this underestimation. Both indicator versions similarly capture the normalization of growth rates in the summer of 2020. The downturns in autumn 2020 and winter 2020/21, as well as the subsequent recovery, were underestimated and delayed by the real-time indicator. Subsequently, both versions show a normalization of growth rates. The 1-month indicator, which incorporates macroeconomic data available within one month, identified these downturns and recoveries earlier than the real-time indicator, but still later than the most recent release. In particular, the 1-month indicator underestimates the downturn and the upturn in 2020, resulting in a faster normalization in autumn 2020. It also overestimates the period in winter 2020/2021, which is the result of a very strong recovery. However, given the large fluctuations in GDP growth, the indicator provides a reasonable picture of weekly GDP growth during this period.

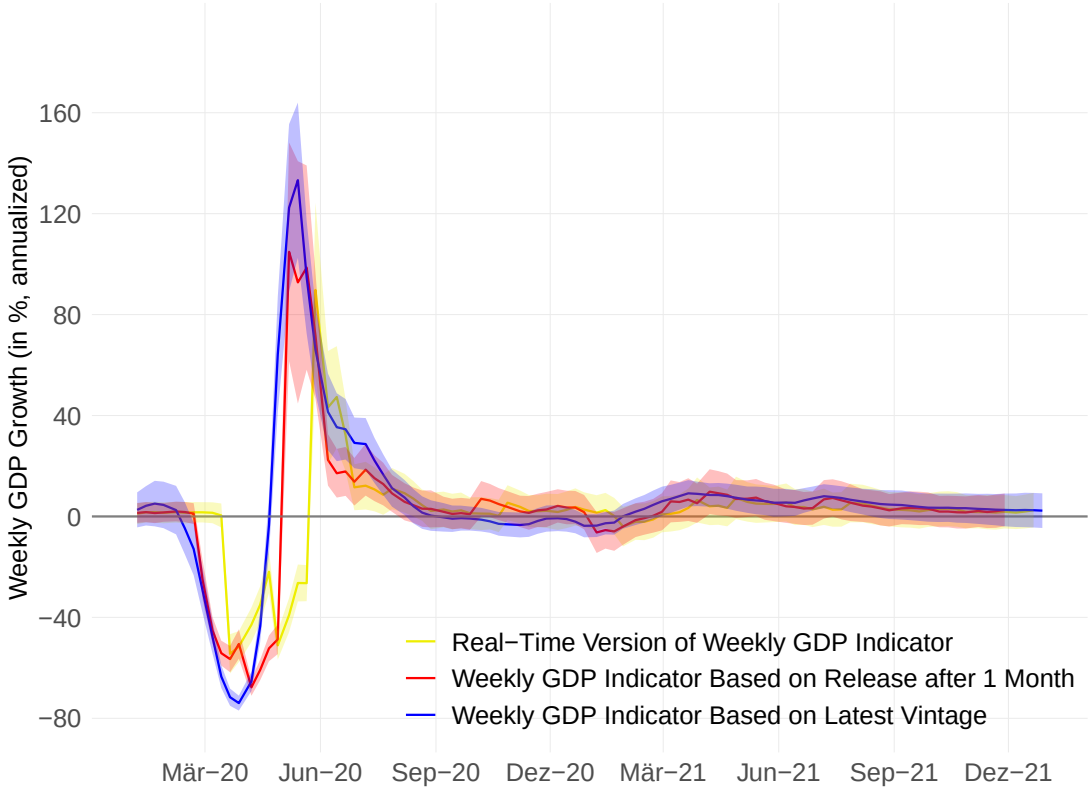

Figure 7: Different Releases of the Weekly GDP Indicator During the COVID-19 Pandemic. The figure compares the weekly GDP indicator as recorded by its first release ("real-time indicator") with the indicator as recorded by its release one month after the first release and with the indicator based on the last available data vintage (December 31, 2021). All indicator versions are displayed with 95%-confidence intervals.

4 Conclusion

This paper introduces a novel weekly GDP indicator for Switzerland, which addresses the limitations of existing economic activity indicators using alternative high-frequency data in capturing rapid and substantial economic shifts observed during the COVID-19 pandemic. The Bayesian mixed-frequency dynamic factor model, which integrates weekly, monthly, and quarterly data from conventional macroeconomic indicators and alternative high-frequency sources, enables near real-time monitoring of GDP.

This paper extends the Bayesian mixed-frequency dynamic factor model proposed by Eckert et al. (2022) to develop a high-frequency indicator that thanks to a straightfor-

ward identification can be interpreted as the weekly quarter-on-quarter GDP growth. The model integrates three independent state-space blocks, estimating missing observations as latent states via data augmentation, extracting dynamic factors, and estimating stochastic volatility in the factor state equation. Additionally, the model addresses serial correlation in the measurement errors by applying quasi-differencing. As a result, the model is able to extract business cycle information from a wide range of data frequencies and capture large and sudden fluctuations.

The empirical application demonstrates that the indicator provides an accurate and timely reflection of Swiss GDP dynamics, offering valuable insights, especially during periods of significant economic disruption. The indicator's performance during economic crisis periods in Switzerland, including the COVID-19 pandemic, illustrates its effectiveness in tracking abrupt economic changes and delivering a credible depiction of these crises. A comparative analysis with other high-frequency indicators for Switzerland highlights the unique utility of this indicator, particularly due to its straightforward interpretation. A pseudo-real-time assessment of the weekly GDP indicator shows that it can identify business cycle turning points at an early stage and quickly converges towards its final version, making it a robust tool for real-time economic analysis.

Bibliography

Adam, T., Michálek, O., Michl, A., and Slezáková, E. (2021). The Rushin index: A weekly indicator of Czech economic activity. *CNB Working Paper*, 2021(4). Czech National Bank (CNB).

Antolin-Diaz, J., Drechsel, T., and Petrella, I. (2024). Advances in nowcasting economic activity: The role of heterogeneous dynamics and fat tails. *Journal of Econometrics*, 238(2):105634.

Aprigliano, V., Emiliozzi, S., Guaitoli, G., Luciani, A., Marcucci, J., and Monteforte, L. (2023). The power of text-based indicators in forecasting italian economic activity. *International Journal of Forecasting*, 39(2):791–808.

Bai, J. and Wang, P. (2015). Identification and Bayesian estimation of dynamic factor models. *Journal of Business & Economic Statistics*, 33(2):221–240.

Baumeister, C., Leiva-León, D., and Sims, E. (2024). Tracking Weekly State-Level Economic Conditions. *The Review of Economics and Statistics*, 106(2):483–504.

Burri, M. and Kaufmann, D. (2020). A daily fever curve for the swiss economy. *Swiss Journal of Economics and Statistics*, 156(1).

Chan, J., Leon-Gonzalez, R., and Strachan, R. W. (2018). Invariant inference and efficient computation in the static factor model. *Journal of the American Statistical Association*, 113(522):819–828.

Chan, J. C. and Jeliazkov, I. (2009). Efficient simulation and integrated likelihood estimation in state space models. *International Journal of Mathematical Modelling and Numerical Optimisation*, 1(1-2):101–120.

Chan, J. C., Poon, A., and Zhu, D. (2023). High-dimensional conditionally gaussian state space models with missing data. *Journal of Econometrics*, 236(1):105468.

Chib, S. and Greenberg, E. (1994). Bayes inference in regression models with ARMA (p, q) errors. *Journal of Econometrics*, 64(1-2):183–206.

Delle Monache, D., Emiliozzi, S., and Nobili, A. (2021). Tracking economic growth during the covid-19: a weekly indicator for italy. *Bank of Italy Note Covid-19, January*.

Eckert, F., Kronenberg, P., Mikosch, H., and Neuwirth, S. (2022). Tracking economic activity with alternative high-frequency data. *SSRN Electronic Journal*.

Eckert, F. and Mikosch, H. (2020). Mobility and sales activity during the corona crisis: Daily indicators for Switzerland. *Swiss Journal of Economics and Statistics*, 156(1):1–10.

Eichenauer, V., Indergand, R., Martinez, I., and Sax, C. (2020). Constructing daily economic sentiment indices based on Google Trends. *KOF Working Papers*, 484. KOF Swiss Economic Institute, ETH Zurich.

Eraslan, S. and Götz, T. (2021). An unconventional weekly economic activity index for Germany. *Economics Letters*, 204:109881.

Eraslan, S. and Reif, M. (2023). A latent weekly gdp indicator for germany. *Technical Paper*, No. 08/2023. Deutsche Bundesbank, Frankfurt a. M.

Felber, L. and Beyeler, S. (2023). Nowcasting economic activity using transaction payments data. *SSRN Electronic Journal*.

Fenz, G. and Stix, H. (2021). Monitoring the economy in real time with the weekly OeNB GDP indicator: Background, experience and outlook. *Monetary Policy & the Economy*, Q4/20-Q1/21:17–40. Oesterreichische Nationalbank (Austrian Central Bank).

Giannone, D., Reichlin, L., and Small, D. (2008). Nowcasting: The real-time informational content of macroeconomic data. *Journal of Monetary Economics*, 55(4):665–676.

Guggia, V., Indergand, R., and Wegmüller, P. (2020). Neuer Index zur wöchentlichen Wirtschaftsaktivität (WWA). *Konjunkturtendenzen SECO Winter 2020/21*.

Kim, S., Shepherd, N., and Chib, S. (1998). Stochastic volatility: Likelihood inference and comparison with ARCH models. *Review of Economic Studies*, 65(3):361–393.

Lewis, D., Mertens, K., and Stock, J. (2020a). U.S. Economic activity during the early weeks of the SARS-CoV-2 outbreak. *NBER Working Paper*, 26954. National Bureau of Economic Research.

Lewis, D. J., Mertens, K., Stock, J. H., and Trivedi, M. (2020b). Measuring real activity using a weekly economic index. *FRB of New York Staff Report*, 920. Federal Reserve Bank of New York.

Lewis, D. J., Mertens, K., Stock, J. H., and Trivedi, M. (2021). Measuring real activity using a weekly economic index. *Journal of Applied Econometrics*, 37(4):667–687.

Mariano, R. S. and Murasawa, Y. (2003). A new coincident index of business cycles based on monthly and quarterly series. *Journal of Applied Econometrics*, 18(4):427–443.

Primiceri, G. E. (2005). Time varying structural vector autoregressions and monetary policy. *Review of Economic Studies*, 72(3):821–852.

Wegmüller, P., Glocker, C., and Guggia, V. (2023). Weekly economic activity: Measurement and informational content. *International Journal of Forecasting*, 39(1):228–243.

Woloszko, N. (2020). Tracking activity in real time with Google trends. *OECD Economics Department Working Papers*, 1634. Organisation for Economic Co-operation and Development (OECD).

Declarations

Availability of data and materials: The datasets used and/or analyzed during the current study are available from the corresponding author on reasonable request.

Competing interests: The author declares that he has no competing interests.

Funding: No third-party funding has been received.

Authors' contributions: The author is solely responsible for the content of this paper.

Acknowledgements: Not applicable

A Government Measures During COVID-19 Pandemic

Table A.1. Chronology of COVID-19 containment measures in Switzerland

Date	Description
28 February 2020	Declaration of "Special Situation" and prohibition of mass events over 1000 people
13 March 2020	Prohibition of events over 100 people, restrictions of maximum occupancy in restaurants, bars,s and clubs. End of classroom teaching.
16 March 2020	Declaration of "Extraordinary Situation": Lockdown and border closures.
20 March 2020	Prohibition of meetings with more than 5 people.
29 April 2020	Shutdown Easing Phase 1: Relaxation of lockdown, opening of shops, restaurants, markets, museums, and gyms. Classroom teaching for children up to the age of 15.
30 May 2020	Meetings with up to 30 people allowed.
06 June 2020	Shutdown Easing Phase 3: Events of up to 300 people allowed. Opening of most leisure and tourism businesses, classroom teaching for all ages.
15 June 2020	Reopening of all borders.
22 June 2020	End of "Extraordinary Situation": Abolition of most containment measures and repealing of home office recommendation.
06 July 2020	Mandatory mask wearing in public transport, quarantine for travelers from high-risk areas.
19 October 2020	Reintroduction of restrictions on meetings with more than 15 people, general mask requirement in public spaces. Home office again recommended.
28 October 2020	Further tightening of restrictions: closure of nightclubs, extension of mandatory mask wearing. Restrictions in restaurants and bars: max. 4 people per group, curfew from 11 PM to 6 AM.
02 November 2020	Ban on in-person events at higher education institutions.
09 December 2020	Ski resorts require approval from the canton and must present strict protection plan.s
12 December 2020	Restricted opening hours for hospitality establishments, public businesses and facilities. Ban on events. Restricted number of people for leisure activities of no more than 5 people.
22 December 2020	Closure of most leisure facilities. Further restriction on the number of people in stores. Expanded use of rapid tests also for asymptomatic individuals.
18 January 2021	Closure of shops selling non-daily necessities. Employers are required to implement home office wherever possible: Masks are mandatory in all indoor work areas.
28 January 2021	The federal government also assumes the costs for tests of asymptomatic individuals.
01 February 2021	Offenses against measures to combat the epidemic are explicitly listed as punishable offenses.
08 February 2021	Possibility of shortening quarantine. Collection of contact details by entering the country. A negative PCR test must be shown upon entering the country.
01 March 2021	Opening of outdoor areas of leisure and sports facilities, shops, museums, and libraries. Private gatherings and events are allowed outdoors with a maximum of 15 people.
15 March 2021	The federal government will cover the costs for all rapid tests
22 March 2021	Private gatherings and events indoors are allowed with a maximum of 10 people.
19 April 2021	Exception from contact quarantine in businesses where testing is conducted. Permitted teaching in-person up to 50 people, and cultural and sporting activities for up to 15 people. Opening of publicly accessible leisure and entertainment facilities. Events are permitted again with restrictions.
31 May 2021	No quarantine for vaccinated and recovered individuals. No mandatory home office for businesses. Relaxation of a maximum number of people for cultural and sports events up to 50 people, private gatherings up to 30 indoors and 50 outdoors, and public events up to 100 and 300. Reopening of indoor areas of restaurants and wellness facilities.
26 June 2021	mask requirement outdoors, home office requirement, attendance limit for in-person events in education facilities and restaurants is lifted. Reopening of nightclubs and dance venues. No restrictions for events where access is limited to individuals with a COVID certificate.
13 September 2021	Certificate requirements for indoor facilities, events, and restaurants, optional at universities and offices.
20 December 2021	Mandatory home office requirement. Cultural and sports activities, indoor events, restaurants, bars, and clubs are restricted to those vaccinated or recovered (2G).

Notes: All information is collected and summarized from official documents from the Swiss Federal Department of Home Affairs FDHA, Federal Office of Public Health FOPH, December 31, 2021.

B Temporal Aggregation

Aggregating the high-frequency factor f_t to a lower frequency factor $\overline{f_t}$ is straightforward for stock variabless. In such scenarios, temporal aggregation is done by simple averaging:

$$\overline{f_t} = \sum_{i=0}^{k-1} \lambda_i f_{t-i}, \quad \text{where} \quad \lambda_i = \frac{1}{k}$$

The variable k indicates how many high frequency intervals fit into a single low frequency interval (e.g., $k = 3$ for aggregating monthly data into quarterly periods). The aggregation becomes more complex for flow variables. These variables are typically used in forecasting models as growth rates, introducing nonlinearities when aggregated over time. Mariano and Murasawa (2003) proposed an approximation using geometric means instead of arithmetic means, which has since become widely adopted:

$$\overline{f_t} = \sum_{i=0}^{s} \lambda_i f_{t-i}, \quad \text{where} \quad \lambda_i = \frac{k - |1 + i - k|}{k}$$

The number of distributed lags is determined by $s = 2(k-1)$. Geometric mean aggregation involves a triangular weighting scheme that addresses the statistical effects observed during the aggregation of growth rates. To illustrate this, consider a flow variable X:

$$\log X_{Q1} = \frac{1}{3} \left(\log X_{Jan} + \log X_{Feb} + \log X_{Mar} \right)$$

The growth rate for the second quarter is determined as:

$$\begin{aligned}
&\log X_{Q2} - \log X_{Q1} = \\
&\quad \frac{1}{3} \Big(\log \left(X_{Jun} + \log X_{May} + \log X_{Apr} \right) - \frac{1}{3} \left(\log X_{Mar} + \log X_{Feb} + \log X_{Jan} \right) \\
&= \frac{1}{3} \left(\log X_{Jun} - \log X_{Mar} \right) + \frac{1}{3} \left(\log X_{May} - \log X_{Feb} \right) + \frac{1}{3} \left(\log X_{Apr} - \log X_{Jan} \right).
\end{aligned}$$

Next, incorporate additional terms into the equation:

$$
\begin{aligned}
&\log X_{Q2} - \log X_{Q1} = \\
&\quad \frac{1}{3}\left(\log X_{Jun} - \log X_{May} + \log X_{May} - \log X_{Apr} + \log X_{April} - \log X_{Mar}\right) + \\
&\frac{1}{3}\left(\log X_{May} - \log X_{Apr} + \log X_{Apr} - \log X_{Mar} + \log X_{Mar} - \log X_{Feb}\right) + \\
&\frac{1}{3}\left(\log X_{Apr} - \log X_{Mar} + \log X_{Mar} - \log X_{Feb} + \log X_{Feb} - \log X_{Jan}\right)
\end{aligned}
$$

By defining growth rates as $x_t = \log X_t - \log X_{t-1}$, the previous equation simplifies to

$$
\begin{aligned}
x_{Q2} =& \frac{1}{3}\left(x_{Jun} + x_{May} + x_{April}\right) + \frac{1}{3}\left(x_{\text{May}} + x_{April} + x_{\text{March}}\right) \\
&+ \frac{1}{3}\left(x_{April} + x_{\text{March}} + x_{Feb}\right) \\
=& \frac{1}{3}x_{Jun} + \frac{2}{3}x_{May} + \frac{3}{3}x_{April} + \frac{2}{3}x_{\text{March}} + \frac{1}{3}x_{Feb}
\end{aligned}
$$

This triangular weighting structure is inserted in the distributed lag matrices $\mathbf{L}_0, \ldots, \mathbf{L}_s$ in Equation (2).

C Estimation

C.1 Latent Data Estimation

To group the parameters in appropriate blocks, the measurement equation for $\mathbf{x}_t$ given in Equation (9) is stacked over all periods $t = 1, \ldots, T$. This results in

$$
\mathbf{y} = \mathbf{S}\mathbf{x} + \boldsymbol{\epsilon}, \qquad \boldsymbol{\epsilon} \sim \mathcal{N}(\mathbf{0}, \mathbf{I}_T \otimes \epsilon \mathbf{I}_n), \tag{11}
$$

where $\mathbf{y} = [\mathbf{y}_1', \ldots, \mathbf{y}_T']'$, $\mathbf{x} = [\mathbf{x}_1', \ldots, \mathbf{x}_T']'$ and $\mathbf{S} = \text{diag}(\mathbf{S}_1, \ldots, \mathbf{S}_T)$. The state equation for $\mathbf{x}_t$, as depicted in Equation (10), is similarly stacked :

$$\mathbf{K}\mathbf{x} = \mathbf{G}\mathbf{f} + \mathbf{u}, \qquad \mathbf{u} \sim \mathcal{N}(\mathbf{0}, \mathbf{I}_T \otimes \mathbf{\Sigma}), \tag{12}$$

with $\mathbf{G}$ defined in Equation (14) and

$$\underset{nT \times nT}{\mathbf{K}} = \begin{bmatrix} \mathbf{I}_n & & & \\ -\boldsymbol{P} & \mathbf{I}_n & & \\ & \ddots & \ddots & \\ & & -\boldsymbol{P} & \mathbf{I}_n \end{bmatrix}.$$

The precision matrix $\mathbf{P}_0$ is then given by $\mathbf{K}'(\mathbf{I}_T \otimes \mathbf{\Sigma})^{-1}\mathbf{K}$ and the conditional posterior of $\mathbf{x}$ follows a normal distribution according to

$$(\mathbf{x}|\mathbf{y}, \mathbf{f}, \mathbf{h}, \mathbf{\Theta}) \sim \mathcal{N}(\mathbf{p}_1, \mathbf{P}_1), \tag{13}$$

with

$$\begin{aligned} \mathbf{P}_1 &= \left(\mathbf{P}_0 + \mathbf{S}'(\mathbf{I}_T \otimes \epsilon\mathbf{I}_n)^{-1})\mathbf{S}\right)^{-1}, \\ \mathbf{p}_1 &= \mathbf{P}_1 \left(\mathbf{K}_{-1}' \left(\mathbf{I}_{T-1} \otimes \mathbf{\Sigma}\right)^{-1} \mathbf{G}\mathbf{f} + \mathbf{S}'(\mathbf{I}_T \otimes \epsilon\mathbf{I}_n)^{-1})\mathbf{y}\right), \end{aligned}$$

where $\mathbf{K}_{-1}$ denotes $\mathbf{K}$ with its first n rows removed. The conditional posterior distribution of $\mathbf{x}$ is thus a weighted average of $\mathbf{y}$ and a projection using $\mathbf{G}\mathbf{f}$. These weights are determined by $\mathbf{S}$, taking values of zero or one. Specifically, when a variable is observed and its corresponding entry in $\mathbf{y}_t$ is non-zero, its weight is one, and the corresponding entry in $\mathbf{x}_t$ approximates this observed value. In contrast, when a variable is not observed and its corresponding entry in $\mathbf{y}_t$ is zero, its weight is zero, and the corresponding entry

in $\mathbf{x}_t$ is equal to the projection estimate.

C.2 Dynamic Factor

To estimate f_t, the measurement equation for the factor, as presented in Equation (5), is stacked over all time periods $t = 1, \ldots, T$, resulting in

$$\tilde{\mathbf{x}} = \mathbf{G}\mathbf{f} + \mathbf{u}, \qquad \mathbf{u} \sim \mathcal{N}(\mathbf{0}, \mathbf{I}_T \otimes \boldsymbol{\Sigma}), \tag{14}$$

where

$$\underset{n(T-1)\times 1}{\tilde{\mathbf{x}}} = \begin{bmatrix} \tilde{\mathbf{x}}_2 \\ \vdots \\ \tilde{\mathbf{x}}_T \end{bmatrix}, \qquad \underset{n(T-1)\times(T+s)}{\mathbf{G}} =$$

$$\begin{bmatrix} -\boldsymbol{\rho}\mathbf{L}_s\boldsymbol{\lambda} & (\mathbf{L}_s - \boldsymbol{\rho}\mathbf{L}_{s-1})\boldsymbol{\lambda} & \ldots & (\mathbf{L}_1 - \boldsymbol{\rho}\mathbf{L}_0)\boldsymbol{\lambda} & \mathbf{L}_0\boldsymbol{\lambda} & \\ & \ddots & & \ddots & & \\ & -\boldsymbol{\rho}\mathbf{L}_s\boldsymbol{\lambda} & (\mathbf{L}_s - \boldsymbol{\rho}\mathbf{L}_{s-1})\boldsymbol{\lambda} & \ldots & (\mathbf{L}_1 - \boldsymbol{\rho}\mathbf{L}_0)\boldsymbol{\lambda} & \mathbf{L}_0\boldsymbol{\lambda} \end{bmatrix}.$$

It should be noted that G incorporates the temporal aggregation scheme of Mariano (2003) into the procedure established by Chan (2009). The state equation for the factor, as presented in Equation (6), is similarly stacked:

$$\mathbf{H}\mathbf{f} = \mathbf{v}, \qquad \mathbf{v} \sim \mathcal{N}(\mathbf{0}, \mathbf{V}), \tag{15}$$

where

$$\underset{(T+s)\times(T+s)}{\mathbf{H}} = \begin{bmatrix} 1 & & & & & & \\ -\phi_1 & 1 & & & & & \\ \vdots & \ddots & \ddots & & & & \\ -\phi_p & \dots & -\phi_1 & 1 & & & \\ & \ddots & \ddots & \ddots & \ddots & & \\ & & -\phi_p & \dots & -\phi_1 & 1 \end{bmatrix}, \qquad \underset{(T+s)\times 1}{\mathbf{f}} = \begin{bmatrix} f_{1-s} \\ f_{2-s} \\ \vdots \\ f_1 \\ \vdots \\ f_T \end{bmatrix},$$

where $\mathbf{V}$ is a diagonal matrix containing the time-varying variances $e^{2h_{1-s}}, \dots, e^{2h_T}$. The precision matrix $\mathbf{F}_0$ is defined as $\mathbf{H}'\mathbf{V}^{-1}\mathbf{H}$. Consequently, the conditional posterior distribution of the factors follows a normal distribution given by

$$\mathbf{f} \sim \mathcal{N}(\mathbf{f}_1, \mathbf{F}_1), \quad \text{where} \quad \mathbf{f}_1 = \mathbf{F}_1 \left(\mathbf{G}'(\mathbf{I}_T \otimes \mathbf{\Sigma}^{-1})\tilde{\mathbf{x}} \right),$$
$$\mathbf{F}_1 = \left(\mathbf{F}_0 + \mathbf{G}'(\mathbf{I}_T \otimes \mathbf{\Sigma}^{-1})\mathbf{G} \right)^{-1}.$$

Rather than inverting $\mathbf{F}_1$, it is more efficient to compute the banded Cholesky factor of $\mathbf{F}_1$ and solve for $\mathbf{f}_1$ using forward and backward substitution. Overall, employing block-banded matrix algorithms significantly enhances the computational efficiency of estimating the latent states f_t, h_t, and $\mathbf{x}_t$, as well as the remaining parameters.

C.3 Factor Loadings

The factor loadings $\boldsymbol{\lambda}$ are estimated by stacking the quasi-differenced measurement equation (5) over all periods $t = 1, \dots, T$. This results in:

$$\tilde{\mathbf{x}} = \mathbf{Z}\boldsymbol{\lambda} + \mathbf{u}, \quad \mathbf{u} \sim \mathcal{N}\left(\mathbf{0}, \mathbf{I}_T \otimes \mathbf{\Sigma}\right), \tag{16}$$

where

$$\underset{n(T-1)\times n}{\mathbf{Z}} = \sum_{i=0}^{s} \begin{bmatrix} \mathbf{f}_{2-i}\mathbf{D}_i \\ \vdots \\ \mathbf{f}_{T-i}\mathbf{D}_i \end{bmatrix}, \quad \mathbf{D}_i = \begin{cases} \mathbf{L}_0, & \text{if } i = 0, \\ -\boldsymbol{P}\mathbf{L}_s, & \text{if } i = s, \\ \mathbf{L}_{i-1} - \boldsymbol{P}\mathbf{L}_i, & \text{otherwise.} \end{cases}$$

This results in the following conditional posterior distribution of the factor loadings:

$$(\boldsymbol{\lambda}|\mathbf{x}, \mathbf{f}, \mathbf{h}, \boldsymbol{\Theta}\backslash\boldsymbol{\lambda}) \sim \mathcal{N}(\mathbf{b}_1, \mathbf{B}_1) \text{ with } \mathbf{B}_1 = \left(\mathbf{B}_0^{-1} + \mathbf{Z}'(\mathbf{I}_{T-1} \otimes \boldsymbol{\Sigma}^{-1})\mathbf{Z}\right)^{-1}, \tag{17}$$
$$\mathbf{b}_1 = \mathbf{B}_1\left(\mathbf{B}_0^{-1}\mathbf{b}_0 + \mathbf{Z}'(\mathbf{I}_{T-1} \otimes \boldsymbol{\Sigma}^{-1})\tilde{\mathbf{x}}\right).$$

The prior mean vector $\mathbf{b}_0$ is a vector of ones. Choosing very large values for the prior variances in $\mathbf{B}_0$ results in an uninformative prior.

C.4 Error Covariance in Factor Measurement Equation

To estimate the covariance matrix $\boldsymbol{\Sigma}$ of the serially uncorrelated measurement errors in the quasi-differenced measurement equation (5), the measurement errors are computed from $\tilde{\mathbf{x}} - \mathbf{Z}\boldsymbol{\lambda}$ are stacked. The matrix $\boldsymbol{\Sigma}$ is assumed to be diagonal, reflecting the belief that the dynamic factor captures most of the cross-correlation in the data. Additionally, the variances of the measurement errors are considered to be constant over time to maintain a simple model structure. Consequently, the error variances σ_i^2 are drawn from an inverse Gamma distribution for each equation.[1]

[1] An alternative model incorporating stochastic volatility in the measurement equation was tested. However, this led to significant numerical instabilities during sampling due to the high frequency of estimation and the inclusion of numerous time series.

$$\sigma_i^2 \sim \mathcal{IG}\left(c_{1,i}/2, d_{1,i}/2\right), \quad \text{where} \quad c_{1,i} = c_{0,i} + T, \qquad (18)$$
$$d_{1,i} = d_{0,i} + \mathbf{u}_i\mathbf{u}_i'.$$

The priors are chosen to be uninformative with $c_{0,i} = 3$ and $d_{0,i} = 10^{-9}$.

C.5 Autoregressive Coefficients of Factor Measurement Errors

The autoregressive coefficients in matrix $\boldsymbol{P}$ of Equation (3) in the main text are estimated from the serially correlated measurement errors of Equation (2) in the main text. These measurement errors are obtained from $\mathbf{x}_t - \mathbf{L}_0\boldsymbol{\lambda}f_t + \mathbf{L}_1\boldsymbol{\lambda}f_{t-1} + \ldots + \mathbf{L}_s\boldsymbol{\lambda}f_{t-s}$ for $t = 1, \ldots, T$. The diagonal elements of $\boldsymbol{P}$ are drawn individually for each equation, based on the vector $\mathbf{e}_i$, which contains the serially correlated errors for the ith variable. The conditional posterior distribution for these diagonal elements, $P_i, \ldots, P_n$, is given by

$$(P_i|\mathbf{x}, \mathbf{f}, \mathbf{h}, \boldsymbol{\Theta}\backslash P_i) \sim \mathcal{N}\left(r_{1,i}, R_{1,i}\right) \text{ with } R_{1,i} = \left(R_{0,i}^{-1} + \sigma_i^{-2}\mathbf{e}_{i,-T}'\mathbf{e}_{i,-T}\right)^{-1}, \qquad (19)$$
$$r_{1,i} = R_{1,i}\left(R_{0,i}^{-1}r_{0,i} + \sigma_i^{-2}\mathbf{e}_{i,-T}'\mathbf{e}_{i,-1}\right).$$

The prior mean $r_{0,i}$ for all variables i is set to 0. The prior variances $R_{0,i}$ are set to $1/T$. This choice is weakly informative and pulls the autoregressive coefficients towards zero.

C.6 Autoregressive Coefficients of Factor State Equation

The autoregressive coefficients $\Phi_1, \ldots, \Phi_p$ are derived according to the method described by Chan et al. (2018). The state equation for the factor in Equation (6) is combined over

all periods from $t = p + 1$ to T to obtain

$$\mathbf{m} = \mathbf{M}\mathbf{\Phi} + \mathbf{v}, \quad \mathbf{v} \sim \mathcal{N}(\mathbf{0}, \mathbf{V}), \tag{20}$$

where

$$\mathbf{m} = \begin{bmatrix} f_{p+1} \\ \vdots \\ f_T \end{bmatrix}, \quad \mathbf{M} = \begin{bmatrix} f_p & \dots & f_1 \\ \vdots & \ddots & \vdots \\ f_{T-1} & \dots & f_{T-p} \end{bmatrix}, \quad \mathbf{\Phi} = \begin{bmatrix} \Phi_1 \\ \vdots \\ \Phi_p \end{bmatrix}$$

with $\mathbf{V}$ being a diagonal matrix containing the time-varying variances of the state equation $e^{2h_{p+1}}, \dots, e^{2h_T}$. The conditional posterior is given by

$$(\mathbf{\Phi}|\mathbf{x}, \mathbf{f}, \mathbf{h}, \mathbf{\Theta}\backslash\mathbf{\Phi}) \sim \mathcal{N}(\mathbf{a}_1, \mathbf{A}_1) \text{ with } \mathbf{A}_1 = \left(\mathbf{A}_0^{-1} + \mathbf{M}'\mathbf{V}^{-1}\mathbf{M}\right)^{-1}, \tag{21}$$
$$\mathbf{a}_1 = \mathbf{A}_1\left(\mathbf{A}_0^{-1}\mathbf{a}_0 + \mathbf{M}'\mathbf{V}^{-1}\mathbf{m}\right).$$

For the chosen parameterization of $p = 1$, priors can be set as uninformative with a mean of zero and a variance of one.[2] Stationarity is enforced by discarding draws where the largest absolute eigenvalue of the companion matrix exceeds a specific threshold. Following the approach in Antolin-Diaz et al. (2024), setting this threshold to 0.8 has been found to ensure robust convergence, thereby promoting stationarity. This threshold enhances the numerical stability of the Gibbs sampling process. After convergence, the draws of $\Phi_1, \dots, \Phi_p$ generally remain well below this threshold.

[2]Higher-order autoregressive processes likely require constraints on the parameter space, such as a prior that forces distant lag parameters towards zero more strongly. In such cases, $\mathbf{a}_0$ would be a vector of zeros, and $\mathbf{A}_0$ would be a diagonal matrix with values of $1/p^2$.

C.7 Error Variance in Stochastic Volatility State Equation

The variance ω of the errors in the state equation for the stochastic volatility factor, as shown in Equation (7), is sampled from an inverse gamma distribution as follows:

$$\omega \sim \mathcal{IG}\left(k_1/2, l_1/2\right), \quad \text{where} \quad k_1 = k_0 + T + s, \qquad (22)$$
$$l_1 = l_0 + \mathbf{v}\mathbf{v}'.$$

The vector $\mathbf{v}$ holds the residuals from the stochastic volatility state equation. Uninformative priors are used, with $k_0 = 3$ and $l_0 = 0.01$.

C.8 Stochastic Volatility

The error term in the measurement equation for the stochastic volatility factor from Equation (8) follows a $\log \chi^2(1)$-distribution. To approximate this within a linear Gaussian state space model, the moments of the distribution are estimated using a mixture of normal distributions, as detailed by Kim et al. (1998) and Primiceri (2005). This approach uses a combination of seven normal distributions. Each distribution $j = 1, \ldots, 7$ has a specific mean μ_j, variance ξ_j, and is selected based on a probability q_j. The parameters and selection probabilities are taken directly from Kim et al. (1998) and are summarized in Table C.2.

Table C.2. Parameters and Selection Probabilities of Mixing Distribution

j	q_j	μ_j	ξ_j
1	0.00730	–11.40039	5.79596
2	0.10556	–5.24321	2.61369
3	0.00002	–9.83726	5.17950
4	0.04395	1.50746	0.16735
5	0.34001	–0.65098	0.64009
6	0.24566	0.52478	0.34023
7	0.25750	–2.35859	1.26261

Notes: $\mu_j + 1.2704$ equals m_i from Table 4 of Kim et al. (1998). .

For simplicity in notation, define $w_t = \log\Big((f_t - \phi_1 f_{t-1} + \ldots + \phi_p f_{t-p})^2 + c\Big)$. To estimate the stochastic volatility factor h_t, the measurement equation for h_t from Equation (8) is stacked over all periods $t = 1, \ldots, T$ to get[3]

$$\mathrm{w} = \mathbf{W}\mathbf{h} - \boldsymbol{\mu} + \varepsilon, \quad \varepsilon \sim \mathcal{N}(\mathbf{0}, \boldsymbol{\Xi})$$

where

$$\underset{(T+s)\times 1}{\mathbf{W}} = \begin{bmatrix} w_{1-s} \\ \vdots \\ w_1 \\ \vdots \\ w_T \end{bmatrix}, \quad \underset{(T+s)\times(T+s)}{\mathbf{W}} = \begin{bmatrix} 2 & & & & \\ & 2 & & & \\ & & \ddots & & \\ & & & 2 & \\ & & & & 2 \end{bmatrix}, \quad \underset{(T+s)\times 1}{\mathbf{h}} = \begin{bmatrix} h_{1-s} \\ \vdots \\ h_1 \\ \vdots \\ h_T \end{bmatrix}$$

Each element of the vector $\boldsymbol{\mu}$ is assigned a specific μ_j from the set $[\mu_1, \ldots, \mu_7]$, according to the probabilities listed in Table C.2. Similarly, each element of the diagonal matrix $\boldsymbol{\Xi}$ is filled with the corresponding ξ_j values from the set $[\xi_1, \ldots, \xi_7]$ as specified in the table.

There is no prior knowledge about the initial state of the stochastic volatility. Therefore, the approach of Chan and Jeliazkov (2009) is followed, imposing a diffuse prior by stacking the stochastic volatility state equation from Equation (7) accordingly:

$$\mathbf{N}\mathbf{h} = \mathbf{u}, \quad \mathbf{u} \sim \mathcal{N}\left(\mathbf{0}, \omega \mathbf{I}_{T+s}\right)$$

[3]Note that no values exist for $w_{1-s}, \ldots, w_{1-s+p-1}$ since f_{1-s} is the first estimated factor. Values for w_t are assumed to be zero.

where $\mathbf{N}$ is of reduced rank and is given by

$$\underset{(T+s-1)\times(T+s)}{\mathbf{N}} = \begin{bmatrix} -1 & 1 & & \\ & \ddots & \ddots & \\ & & -1 & 1 \end{bmatrix}$$

The precision matrix $\mathbf{Q}_0$ is defined as $\mathbf{N}'\left(\omega \mathbf{I}_{T+s}\right)^{-1}\mathbf{N}$ and the conditional posterior of the stochastic volatility is normally distributed:

$$\mathbf{h} \sim \mathcal{N}\left(\mathbf{q}_1, \mathbf{Q}_1\right) \quad \text{where} \quad \mathbf{Q}_1 = \left(\mathbf{Q}_0 + \mathbf{W}'\boldsymbol{\Xi}^{-1}\mathbf{W}\right)^{-1}$$
$$\mathbf{q}_1 = \mathbf{Q}_1\left(\mathbf{W}'\boldsymbol{\Xi}^{-1}(\mathbf{w} + \boldsymbol{\mu})\right)$$

Similarly to the dynamic factor, this algorithm becomes computationally highly efficient when utilizing block-banded matrix algorithms and preallocating sparse matrices.

KOF

ETH Zurich
KOF Swiss Economic Institute
LEE G 116
Leonhardstrasse 21
8092 Zurich, Switzerland

Phone +41 44 632 42 39
kof@kof.ethz.ch
www.kof.ch